The American Journal of Pathology, Vol. 169, No. 6, December 2006

DOI: 10.2353/ajpath.2006.060329

Musculoskeletal Pathology

Genetic Ablation of Vitamin D Activation Pathway Reverses Biochemical and Skeletal Anomalies in *Fgf-23*-Null Animals

Despina Sitara,* Mohammed S. Razzaque,* René St-Arnaud,† Wei Huang,* Takashi Taguchi,‡ Reinhold G. Erben,§ and Beate Lanske*

From the Department of Developmental Biology, Harvard School of Dental Medicine, Boston, Massachusetts; the Genetics Unit,† Shriners Hospital, Montreal, Quebec, Canada; the Department of Pathology,‡ Nagasaki University Graduate School of Biomedical Sciences, Nagasaki, Japan; and the Department of Natural Sciences,§ University of Veterinary Medicine, Vienna, Austria*

Fibroblast growth factor-23 (FGF-23) is one of the circulating phosphaturic factors associated with renal phosphate wasting. *Fgf-23*$^{-/-}$ animals show extremely high serum levels of phosphate and 1,25-dihydroxyvitamin D_3, along with abnormal bone mineralization and soft tissue calcifications. To determine the role of vitamin D in mediating altered phosphate homeostasis and skeletogenesis in the *Fgf-23*$^{-/-}$ mice, we generated mice lacking both the *Fgf-23* and *1α-hydroxylase* genes (*Fgf-23*$^{-/-}$/*1α(OH)ase*$^{-/-}$). In the current study, we have identified the cellular source of *Fgf-23* in adult mice. In addition, loss of vitamin D activities from *Fgf-23*$^{-/-}$ mice reverses the severe hyperphosphatemia to hypophosphatemia, attributable to increased urinary phosphate wasting in *Fgf-23*$^{-/-}$/*1α(OH)ase*$^{-/-}$ mice, possibly as a consequence of decreased expression of NaPi2a. Ablation of vitamin D from *Fgf-23*$^{-/-}$ mice resulted in further reduction of total bone mineral content and bone mineral density and reversed ectopic calcification of skeleton and soft tissues, suggesting that abnormal mineral ion homeostasis and impaired skeletogenesis in *Fgf-23*$^{-/-}$ mice are mediated through enhanced vitamin D activities. In conclusion, using genetic manipulation studies, we have provided evidence for an *in vivo* inverse correlation between Fgf-23 and vitamin D activities and for the severe skeletal and soft tissue abnormalities of *Fgf-23*$^{-/-}$ mice being mediated through vitamin D. *(Am J Pathol 2006, 169:2161–2170; DOI: 10.2353/ajpath.2006.060329)*

Maintenance of delicate phosphate homeostasis is not only essential for normal skeletogenesis but also for preservation of normal bone integrity. Regulation of phosphate homeostasis is a complex hormonal process, involving multiple organs, including intestine, kidney, bone, and parathyroid glands. The skeletal defects of phosphate deprivation or wasting are probably attributable to a negative phosphate balance at the bone level, ie, lack of phosphate-deposition and or phosphate-mobilization from bone in the growing skeleton.

In contrast, prolonged hyperphosphatemia induces excessive skeletal mineral deposition with widespread soft tissue calcifications and atherosclerosis. Until recently, phosphate homeostasis was thought to be passively mediated by molecules that are involved in regulating calcium homeostasis by exerting inverse effects on serum phosphate.[1] However, detailed analyses of rare genetic disorders including tumor-induced osteomalacia,[2] autosomal dominant hypophosphatemic rickets,[3] and X-linked hypophosphatemia[4] have led to the identification of various key molecules involved specifically in the regulation of phosphate homeostasis; one such identified molecule is FGF-23.[2] Subsequently, studies using genetically engineered mice have provided more insights into the role of FGF-23 in phosphate homeostasis and skeletogenesis. Transgenic mice expressing *FGF-23* under the control of assorted promoters exhibited rickets and osteomalacia caused by renal phosphate wasting but unchanged serum levels of calcium and 1,25-dihydroxyvitamin D_3 [1,25$(OH)_2D_3$].[5–7] In contrast, *Fgf-23*-null (*Fgf-23*$^{-/-}$) mice showed severe hyperphosphatemia, highly elevated serum 1,25$(OH)_2D_3$ levels,[8,9] and ectopic calcifications, resembling the human disease familial tumoral calcinosis.[10–14] All above-mentioned studies suggest a possible role for FGF-23 in maintaining phosphate homeostasis and skeletogenesis.

Supported by funds from the Harvard School of Dental Medicine (to B.L.).

Accepted for publication September 6, 2006.

Address reprint requests to Beate Lanske, Ph.D., Department of Developmental Biology, Harvard School of Dental Medicine, REB 303, 188 Longwood Ave., Boston, MA 02115. E-mail: beate_lanske@hsdm.harvard.edu.

Vitamin D is another known factor that is important in regulation of calcium and phosphate homeostasis and skeletogenesis.[1,15–17] $1,25(OH)_2D_3$, the most active metabolite, is formed in the kidney by hydroxylation through the 1α-hydroxylase. Hence, by altering the activity of the 1α(OH)ase enzyme, the effects of $1,25(OH)_2D_3$ can be modified and thereby change the degree of intestinal phosphate absorption and skeletal mineralization.[18,19] Vitamin D deficiency is a well-known cause of rickets,[20] whereas elevated levels of vitamin D can lead to increased calcium absorption, hypercalcemia, and abnormal soft tissue calcifications. A number of studies have suggested the importance of vitamin D actions in phosphate homeostasis and skeletal mineralization.[15–17,19–30] For instance, *1α(OH)ase*$^{-/-}$ mice show severe secondary hyperparathyroidism with hypocalcemia, hypophosphatemia, and rickets,[19,21,22,31] whereas treatment with $1,25(OH)_2D_3$ or administration of a high-calcium/high-phosphate diet rescued the skeletal phenotype of *1α(OH)ase*$^{-/-}$ mice.[18,21,22,31]

Fgf-23$^{-/-}$ mice have shown significantly elevated levels of serum $1,25(OH)_2D_3$, associated with increased renal expression of the *1α(OH)ase* gene.[8,9] Therefore, the hyperphosphatemia, excessive skeletal mineralization, and soft tissue calcifications in *Fgf-23*$^{-/-}$ mice may be mediated through increased activity of vitamin D. To test this hypothesis, we established a new mouse model, genetically ablated for both *Fgf-23* and *1α(OH)ase*, to determine whether altered phosphate homeostasis and abnormal skeletogenesis in *Fgf-23*$^{-/-}$ mice is a vitamin D-mediated process.

Materials and Methods

Animals

Heterozygous *Fgf-23*, *1α(OH)ase*, and *NaPi2a* mice were interbred at 5 to 12 weeks to attain wild-type, *Fgf-23*$^{-/-}$, *Fgf-23*$^{-/-}$*/1α(OH)ase*$^{-/-}$, *1α(OH)ase*$^{-/-}$, *NaPi2a*$^{-/-}$, and *Fgf-23*$^{-/-}$*/NaPi2a*$^{-/-}$ animals. Routine polymerase chain reaction (PCR) was used to identify *Fgf-23*$^{-/-}$ and *NaPi2a*$^{-/-}$ mice as described previously.[9,32] Genotyping of *1α(OH)ase*$^{-/-}$ animals was performed using the following primers and conditions (forward: 5′-GTCCCAGACAGAGACATCCGT-3′; reverse: 5′-GCACCTGGCTCAGGTAGCTCTTC-3′; annealing at 60°C for 30 seconds, 35 cycles; wild-type, 990 bp; mutant, 345 bp). All studies performed were approved by the institutional care and use committee at the Harvard School of Dental Medicine.

LacZ Staining

The pattern of *Fgf-23* expression was obtained through β-galactosidase staining of *Fgf-23*$^{+/-}$ and *Fgf-23*$^{-/-}$ animals, in a *Hyp* mouse background at 6 weeks postnatally as described previously.[9] All mice stained for lacZ were females, heterozygous for the *Phex* mutation (*Hyp*$^{+/-}$), and heterozygous or homozygous for *Fgf-23*. Stained specimens were embedded in OCT (optimal cutting temperature) medium, and 6-μm frozen sections were cut using a Leica CM3000 microtome (Wetzlar, Germany), to determine cellular expression of *Fgf-23*.

X-Rays and Bone Densitometry

X-rays, bone mineral density (BMD), bone mineral content (BMC), and peripheral quantitative computed tomography (pQCT) were determined in 6-week-old mice as described previously.[9]

Biochemical Analysis

Blood was obtained by heart puncture or retro-orbital bleeding of 5- to 12-week-old animals. Serum phosphorus and total serum calcium were determined using Stanbio LiquiUV and LiquiColor (Arsenazo III) kits (Stanbio Laboratory, Boerne, TX), respectively. Urinary phosphorus and creatinine were determined using Stanbio LiquiUV and creatinine kits, respectively. Serum PTH and Fgf-23 levels were measured using a mouse intact parathyroid hormone (PTH) (Immunotopics, San Clemente, CA) and a serum FGF-23 (Kainos Laboratories, Inc., Tokyo, Japan) enzyme-linked immunosorbent assay kit, respectively.

Mineralization

The mineralization pattern of the skeleton was analyzed in 6-week-old mice as described earlier by McLeod.[33] Soft tissues were fixed in 10% buffered formalin, embedded in paraffin, sectioned, and stained for von Kossa as described previously.[34]

Histological Analysis

For histological analyses, paraffin and methylmethacrylate sections of bones were prepared at 6 weeks postnatally as described previously.[9,35] To examine frozen *lacZ* sections, stained tissues were demineralized in 0.5 mol/L ethylenediaminetetraacetic acid for 10 days, rinsed in phosphate-buffered saline (PBS), embedded in OCT medium, serially sectioned at 6 μm, and counterstained with eosin. Soft tissues were fixed either in Carnoy's solution or in 10% formalin and routinely processed and embedded in paraffin, cut into 4-μm-thick sections, and stained with hematoxylin and eosin and von Kossa.

In Situ *Hybridization*

Complementary ^{35}S-UTP-labeled riboprobes (complementary RNAs for collagen type X, collagen type II, osteopontin, matrix gla protein) were used for performing *in situ* hybridization on paraffin sections, as described previously.[34]

Immunofluorescence Staining for NaPi2a

Immunostaining was performed as described previously.[36] In brief, PLP (1%, phosphate/lysine/paraformaldehyde)-fixed tissues were stored at −80°C and embedded in OCT, and frozen sections were prepared for further

staining. Frozen sections were incubated with blocking solution for 30 minutes and then overnight with polyclonal anti-NaPi2a antibody (dilution 1:100; Alpha Diagnostic, San Antonio, TX) at 4°C. The slides were washed with PBS and incubated with fluorescein isothiocyanate-leveled anti-rabbit secondary antibody (dilution, 1:100) for 30 minutes. After PBS wash, coverslips were placed on slides using 4,6-diamidino-2-phenylindole (DAPI)-containing mounting media, and antibody binding was visualized under UV light, using immunofluorescence microscopy. Rabbit serum or PBS, instead of primary antibody, was used as negative control.

Statistics

Statistically significant differences between groups were evaluated by Student's *t*-test for comparison between two groups or by one-way analysis of variance followed by Tukey's test for multiple comparisons. All values were expressed as mean ± SE. A P value of less than 0.05 was considered to be statistically significant. All analyses were performed using Microsoft Excel and GraphPad Prism 4.0.

Results

Postnatal Expression of Fgf-23

We have previously reported the generation of *Fgf-23*$^{-/-}$ animals, in which we replaced the entire coding region with the lacZ gene.[9] Because *Fgf-23* gene expression is at low abundance, it is difficult to determine its cellular sources. In this study, we have taken advantage of up-regulated expression of *Fgf-23* in *Hyp* animals and crossed *Fgf-23*$^{+/-}$ animals into the *Hyp* mouse background to perform *lacZ* staining of *Hyp*$^{+/-}$*/Fgf-23* double-mutant female animals at 6 weeks. Positive β-galactosidase staining was only detected in the skeleton of these animals, suggesting that bone is one of the major sources of *Fgf-23* production after birth (Figure 1A). No staining was obvious in any of the soft tissues, probably attributable to low abundance of *Fgf-23* gene expression in these tissues. Moreover, no such staining was detected in bones of control littermates even after an extended 8-hour period of staining. To determine the distribution of *Fgf-23*-producing cells, frozen sections were prepared from various lacZ-stained skeletal tissues and were analyzed by routine light microscope (Figure 1B). *Fgf-23* expression was mostly evident in osteocytes of *Hyp*$^{+/-}$*/Fgf-23* double mutants; however, not all osteocytes were found to be stained positively. To test whether osteoblasts could also express *Fgf-23*, we performed *in vitro* calvarial cultures and were unable to detect *Fgf-23* expression in these cells, either by *lacZ* staining or by real-time PCR (data not shown).

Generation of Fgf-23$^{-/-}$*/1α (OH)ase*$^{-/-}$ *Compound Mutants*

Our previous study[9] has shown that *in vivo* ablation of *Fgf-23* results in severe hyperphosphatemia and severe

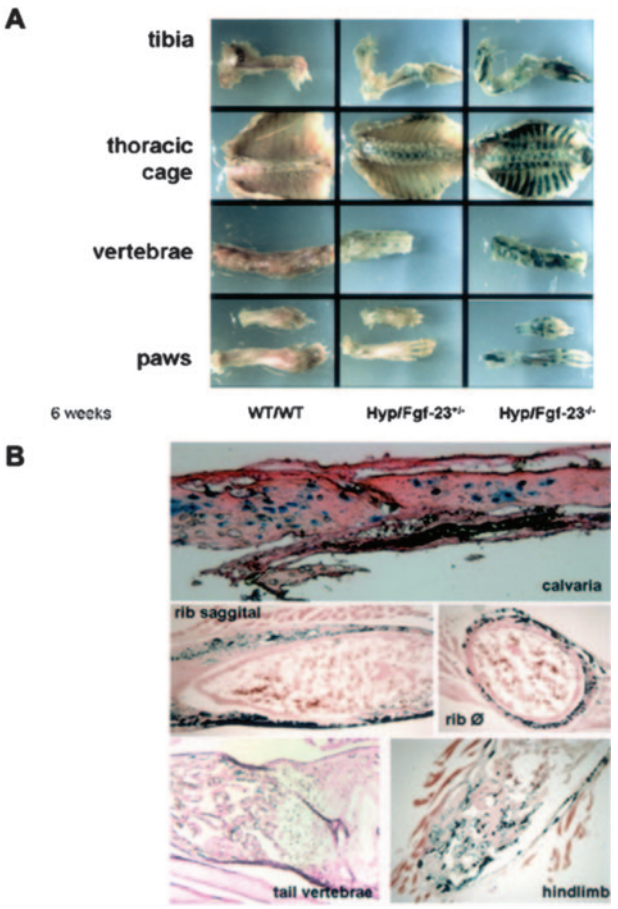

Figure 1. Expression of *Fgf-23* by β-galactosidase staining at 6 weeks. **A:** Shown are various skeletal elements including tibia, thoracic cage, vertebrae, and paws of wild-type (WT/WT) mouse, an *Fgf-23* heterozygous mouse in a *Hyp* mouse background (*Hyp*$^{+/-}$*/Fgf-23*$^{+/-}$), and an *Fgf-23* homozygous mutant mouse in a *Hyp* mouse background (*Hyp*$^{+/-}$*/Fgf-23*$^{-/-}$). Please note the difference in intensity of β-galactosidase staining in *Hyp*$^{+/-}$*/Fgf-23*$^{+/-}$ versus *Hyp*$^{+/-}$*/Fgf-23*$^{-/-}$ bones. **B:** Represented are frozen sections of stained *Hyp*$^{+/-}$*/Fgf-23*$^{-/-}$ bones such as calvaria, ribs (saggital and transverse), tail vertebrae, and tibia/hindlimb; specific blue staining is only evident in osteocytes of intramembranous and endochondral formed bones. No staining is evident in osteoblasts or cartilaginous areas.

increase in serum levels of the active vitamin D hormone. Elevated serum 1,25$(OH)_2D_3$ levels are associated with significant renal up-regulation of the *1α(OH)ase* gene.[37] To test the hypothesis that Fgf-23-regulated alteration of phosphate homeostasis, excessive skeletal mineralization, and soft tissue calcification in *Fgf-23*$^{-/-}$ mice are partly mediated through increased vitamin D activity, we generated *Fgf-23*$^{-/-}$*/1α(OH)ase*$^{-/-}$ compound mutants. In the current study, we compared and analyzed data obtained from wild-type, *Fgf-23*$^{-/-}$, *Fgf-23*$^{-/-}$*/1α(OH)ase*$^{-/-}$, and *1α(OH)ase*$^{-/-}$ animals.

Macroscopic Characterization of Fgf-23$^{-/-}$*/1α(OH)ase*$^{-/-}$ *Double Mutants*

At birth, *Fgf-23*$^{-/-}$*/1α(OH)ase*$^{-/-}$ mice appear indistinguishable from other littermates. Three weeks after birth, *Fgf-23*$^{-/-}$*/1α(OH)ase*$^{-/-}$ compound mutants appear

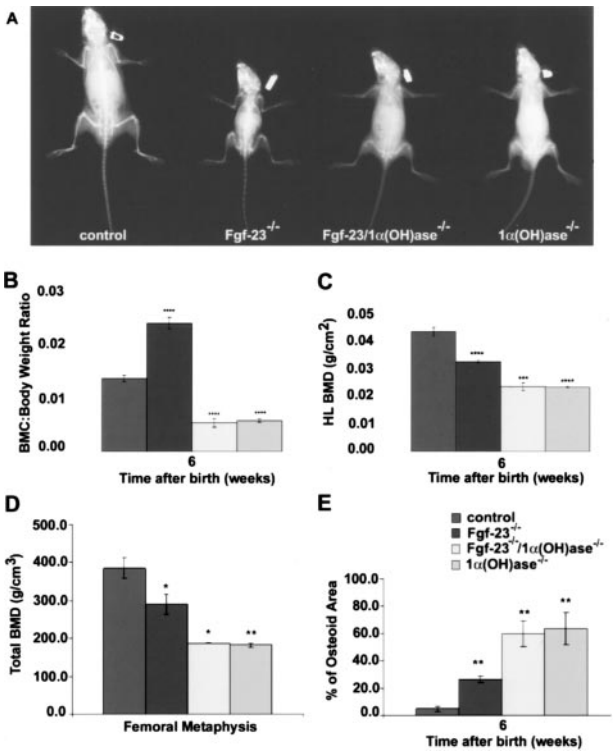

Figure 2. A: X-ray autoradiography of total skeletons of a control, *Fgf-23*$^{-/-}$, *Fgf-23*$^{-/-}$*/1α(OH)ase*$^{-/-}$, and *1α(OH)ase*$^{-/-}$ animal at 6 weeks. **B–D:** Total BMC (**B**, each value obtained for BMC was normalized to the body weight of the corresponding animal), and BMD (**C** and **D**) by PIXImus and pQCT of hindlimbs of control, *Fgf-23*$^{-/-}$, *Fgf-23*$^{-/-}$*/1α(OH)ase*$^{-/-}$, and *1α(OH)ase*$^{-/-}$ animals are shown. **E:** Quantitative histomorphometry on osteoid volume of control, *Fgf-23*$^{-/-}$, *Fgf-23*$^{-/-}$*/1α(OH)ase*$^{-/-}$, and *1α(OH)ase*$^{-/-}$ animals (statistical significance: *$P < 0.05$, **$P < 0.01$,***$P < 0.001$, ****$P < 0.0001$). There was no statistical significant difference between WT (*Fgf-23*$^{+/+}$*/1α(OH)ase*$^{+/+}$) and *Fgf-23*$^{+/-}$*/1α(OH)ase*$^{+/-}$, *Fgf-23*$^{-/-}$ and *Fgf-23*$^{-/-}$*/1α(OH)ase*$^{+/-}$, and *Fgf-23*$^{-/-}$*/1α(OH)ase*$^{-/-}$ and *1α(OH)ase*$^{-/-}$*/Fgf-23*$^{+/-}$ animals, so data were combined.

slightly smaller than wild-type and are similar to *1α(OH)ase*$^{-/-}$ single knockout animals. Apart from the slightly reduced body size, double mutants do not show any obvious abnormalities, having normal physical activities, when compared with the severely weakened *Fgf-23*$^{-/-}$ littermates.

X-Ray Analyses and Bone Densitometry

To evaluate the effects of *1α(OH)ase* gene ablation on the skeleton of *Fgf-23*$^{-/-}$ animals, X-ray images were taken from control, *Fgf-23*$^{-/-}$, *Fgf-23*$^{-/-}$*/1α(OH)ase*$^{-/-}$, and *1α(OH)ase*$^{-/-}$ littermates at 6 weeks (Figures 2A and 4A). Bones of double mutants were short and thick and showed the typical features of rickets such as widening of the epiphysis and cupping of the metaphysis, resembling the phenotype of *1α(OH)ase*$^{-/-}$ single knockouts. Furthermore, morphological and densitometric measurements using PIXImus and pQCT analyses were performed. All genotypes (wild-type, *Fgf-23*$^{+/-}$*/1α(OH)ase*$^{+/-}$, *Fgf-23*$^{-/-}$, *Fgf-23*$^{-/-}$*/1α(OH)ase*$^{+/-}$, *Fgf-23*$^{-/-}$*/1α(OH)ase*$^{-/-}$, *1α(OH)ase*$^{-/-}$, and *1α(OH)ase*$^{-/-}$*/Fgf-23*$^{+/-}$) were analyzed. Because we could not find any statistically significant difference in the obtained values between wild-type and *Fgf-23*$^{+/-}$*/1α(OH)ase*$^{+/-}$, *Fgf-23*$^{-/-}$ and *Fgf-23*$^{-/-}$*/1α(OH)ase*$^{+/-}$, or *1α(OH)ase*$^{-/-}$ and *1α(OH)ase*$^{-/-}$*/Fgf-23*$^{+/-}$ animals, we have only presented data from four major genotypes: 1) wild-type (control), 2) *Fgf-23* knockout (*Fgf-23*$^{-/-}$), 3) *Fgf-23/1α(OH)ase* double-knockout (*Fgf-23*$^{-/-}$*/1α(OH)ase*$^{-/-}$), and 4) *1α(OH)ase* knockout (*1α(OH)ase*$^{-/-}$) mice. Total body BMC in control, *Fgf-23*$^{-/-}$, *Fgf-23*$^{-/-}$*/1α(OH)ase*$^{-/-}$, and *1α(OH)ase*$^{-/-}$ littermates was analyzed at 6 weeks. In contrast to the significant increase in BMC in *Fgf-23*$^{-/-}$ mice when compared with control (0.024 ± 0.001 versus 0.014 ± 0.0005), the BMC of both *Fgf-23*$^{-/-}$*/1α(OH)ase*$^{-/-}$ (0.005 ± 0.0008) compound mutants and *1α(OH)ase*$^{-/-}$ (0.006 ± 0.0003) animals exhibited a significant decrease (Figure 2B). We further analyzed the BMD of hindlimbs in these animals (Figure 2C) by PIXImus and confirmed the decreased BMD in *Fgf-23*$^{-/-}$ animals (0.032 ± 0.0006 versus 0.043 ± 0.0015 g/cm^2 in control animals). Moreover, we found an additional reduction in BMD in hindlimbs of *Fgf-23*$^{-/-}$*/1α(OH)ase*$^{-/-}$ (0.023 ± 0.001 g/cm^2) and *1α(OH)ase*$^{-/-}$ (0.023 ± 0.0002 g/cm^2) animals when compared with *Fgf-23*$^{-/-}$ mice, suggesting that loss of vitamin D activity leads to severely impaired bone mineralization in *Fgf-23*$^{-/-}$ mice. We extended our measurements by pQCT (Figure 2D) and corroborated our previous observations by PIXImus. Measurements by pQCT demonstrated that femoral volumetric BMD was statistically significantly lower in *Fgf-23*$^{-/-}$, *1α(OH)ase*$^{-/-}$ mutants, and also in *Fgf-23*$^{-/-}$*/1α(OH)ase*$^{-/-}$ double mutants compared with wild-type mice (Figure 2D).

Measurements in Serum and Urine

Serum phosphate, calcium, and parathyroid hormone (PTH) levels for all possible genotypes were assessed in 5- to 12-week-old mice. As reported earlier,[9] *Fgf-23*$^{-/-}$ mice were severely hyperphosphatemic (14.9 ± 0.4 mg/dl) when compared with control littermates (8.2 ± 0.2 mg/dl). In contrast, Fgf-*23*$^{-/-}$*/1α(OH)ase*$^{-/-}$ animals were hypophosphatemic with significantly lower serum phosphate levels (6.2 ± 0.3 mg/dl), comparable with those found in *1α(OH)ase*$^{-/-}$ animals (6 ± 0.4 mg/dl), suggesting that 1,25$(OH)_2D_3$ is an important mediator of controlling phosphate homeostasis in *Fgf-23*$^{-/-}$ mice. Furthermore, *Napi2a*$^{-/-}$ and *Fgf-23*$^{-/-}$*/Napi2a*$^{-/-}$ double mutants showed significantly decreased serum phosphate levels (5.4 ± 0.1 mg/dl and 5.4 ± 0.9 mg/dl), when compared with the ones of *Fgf-23*$^{-/-}$ mice, and were comparable with the ones of Fgf-*23*$^{-/-}$*/1α(OH)ase*$^{-/-}$ animals (Figure 3C). More importantly, decreased urinary phosphate excretion in *Fgf-23*$^{-/-}$ mice was completely reversed in *Fgf-23*$^{-/-}$*/1α(OH)ase*$^{-/-}$ double-mutant animals, which showed severe hyperphosphaturia comparable with that in *1α(OH)ase*$^{-/-}$ mice (Figure 3D).

Furthermore, we quantified serum levels of Fgf-23 in control, *1α(OH)ase*$^{-/-}$, *Hyp*, and *Coll I-FGF23* transgenic mice. In contrast to the extremely high Fgf-23 levels found in *Hyp* and *FGF23* transgenic animals, no measur-

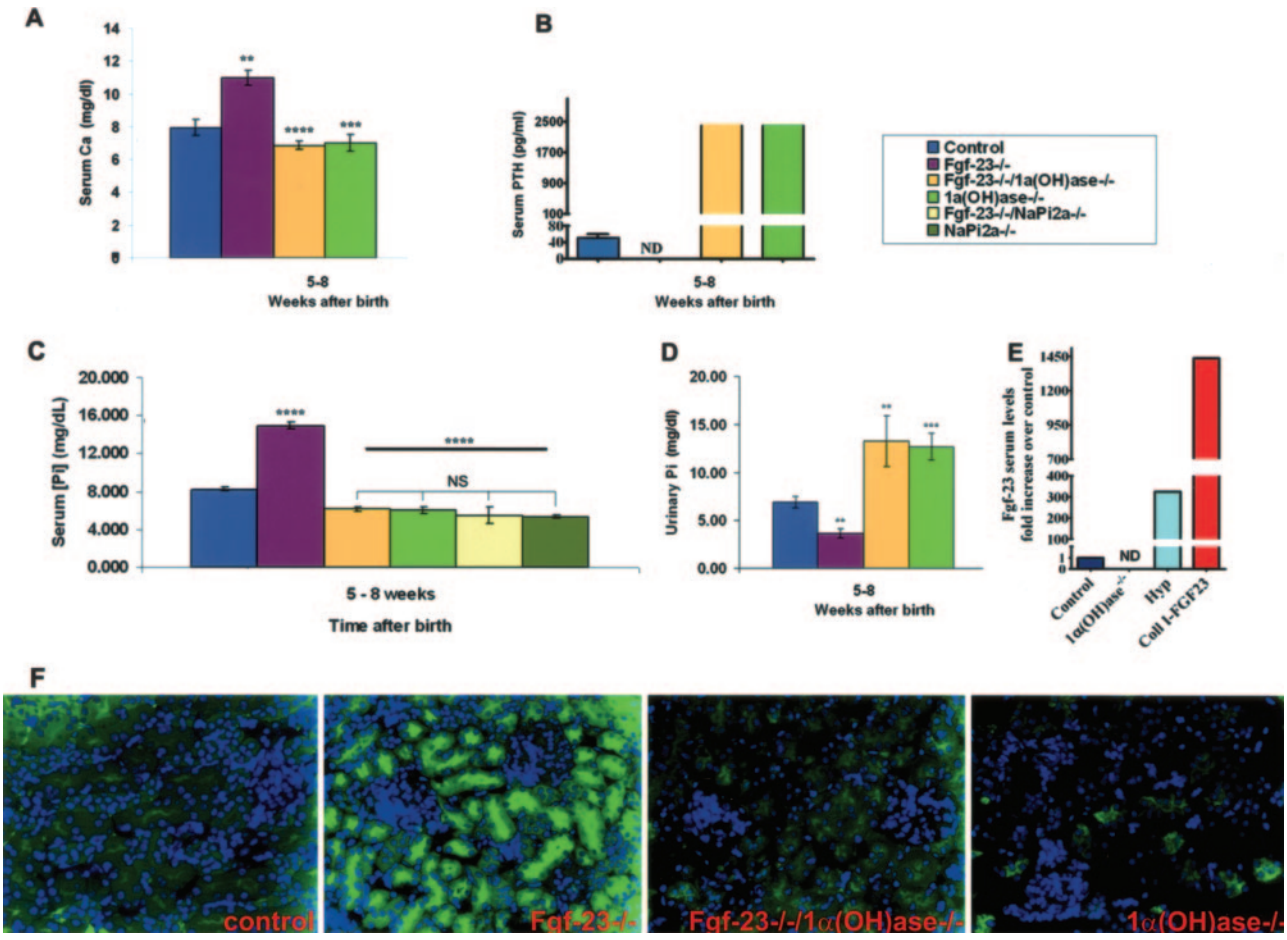

Figure 3. Biochemical measurements of calcium, phosphate, PTH, and FGF-23 (**A–E**), and NaPi2a immunohistochemistry in various mouse mutants (**F**). Serum calcium (**A**) levels in control ($n = 15$), *Fgf-23*$^{-/-}$ ($n = 6$), *Fgf-23*$^{-/-}$/*1α(OH)ase*$^{-/-}$ ($n = 8$), and *1α(OH)ase*$^{-/-}$ ($n = 11$) animals; serum PTH (**B**) levels in control ($n = 8$), *Fgf-23*$^{-/-}$ ($n = 4$), *Fgf-23*$^{-/-}$/*1α(OH)ase*$^{-/-}$ ($n = 3$), and *1α(OH)ase*$^{-/-}$ ($n = 9$) animals; serum phosphate (**C**) levels in control ($n = 22$), *Fgf-23*$^{-/-}$ ($n = 11$), *Fgf-23*$^{-/-}$/*1α(OH)ase*$^{-/-}$ ($n = 7$), *1α(OH)ase*$^{-/-}$ ($n = 14$), *Fgf-23*$^{-/-}$/*NaPi2a*$^{-/-}$ ($n = 3$), and *NaPi2a*$^{-/-}$ ($n = 3$) animals; urinary phosphate (**D**) control ($n = 9$), *Fgf-23*$^{-/-}$ ($n = 5$), *Fgf-23*$^{-/-}$/*1α(OH)ase*$^{-/-}$ ($n = 5$), and *1α(OH)ase*$^{-/-}$ ($n = 9$) animals; and serum Fgf-23 (**E**) levels in control ($n = 8$), *1α(OH)ase*$^{-/-}$ ($n = 5$), *Hyp* (light blue, $n = 1$), and *Coll I-FGF23* (red, $n = 2$) animals were measured in 5- to 12-week-old mice. Statistical significance: $^{**}P < 0.01$, $^{***}P < 0.001$, $^{****}P < 0.0001$. Immunostaining of NaPi2a in the kidney sections prepared from wild-type, *Fgf-23*$^{-/-}$, *Fgf-23*$^{-/-}$/*1α(OH)ase*$^{-/-}$, and *1α(OH)ase*$^{-/-}$ animals using a polyclonal antibody (**F**). Please note that in contrast to the increased expression of NaPi2a in *Fgf-23*$^{-/-}$ mice, there is significantly less expression of NaPi2a protein in the *Fgf-23*$^{-/-}$/*1α(OH)ase*$^{-/-}$ mice, similar to the expression in mice that lack the 1α(OH)ase gene [*1α(OH)ase*$^{-/-}$].

able amounts of Fgf-23 could be detected in *1α(OH)ase* ablated mice when compared with control mice (Figure 3E), reiterating earlier observations that vitamin D is a potent stimulator of Fgf-23 production.

In contrast to the hypercalcemia detected in *Fgf-23*$^{-/-}$ mice (11.0 ± 0.4 mg/dl), serum calcium concentrations of *Fgf-23*$^{-/-}$/*1α(OH)ase*$^{-/-}$ compound mutants were significantly reduced (6.9 ± 0.25 mg/dl) and similar to those obtained from *1α(OH)ase*$^{-/-}$ animals (7.0 ± 0.5 mg/dl) (Figure 3A), leading to secondary hyperparathyroidism as demonstrated by the extremely high levels of serum PTH (Figure 3B). This data would suggest that suppression of PTH production in *Fgf-23*$^{-/-}$ animals is attributable to the hypercalcemia and high $1,25(OH)_2D_3$ serum levels.

Renal Expression of NaPi2a

To determine the role of NaPi2a in *Fgf-23*$^{-/-}$ mice, we examined its expression pattern in kidney sections prepared from wild-type, *Fgf-23*$^{-/-}$, *Fgf-23*$^{-/-}$/*1α(OH)ase*$^{-/-}$, and *1α(OH)ase*$^{-/-}$ animals using a polyclonal NaPi2a antibody. We found increased NaPi2a protein expression in the luminal side of the proximal tubules of *Fgf-23*$^{-/-}$ animals (Figure 3F) when compared with wild-type. In contrast to the NaPi2a expression in *Fgf-23*$^{-/-}$ mice, a markedly decreased expression was detected in *Fgf-23*$^{-/-}$/*1α(OH)ase*$^{-/-}$ mice, similar to the expression of *1α(OH)ase*$^{-/-}$ mice (Figure 3F), suggesting a major contribution of NaPi2a to regulate the hyperphosphatemia consistently found in *Fgf-23*$^{-/-}$ mice.

Mineralization

To examine the mineralization pattern of bones, Alizarin Red S-stained full-body skeletons of *Fgf-23*$^{-/-}$/*1α(OH)ase*$^{-/-}$ mutants were compared with the ones of wild-type, *Fgf-23*$^{-/-}$, and *1α(OH)ase*$^{-/-}$ animals. Double mutants did not exhibit the ectopic bone nodules usually found in *Fgf-23*$^{-/-}$ animals but displayed the

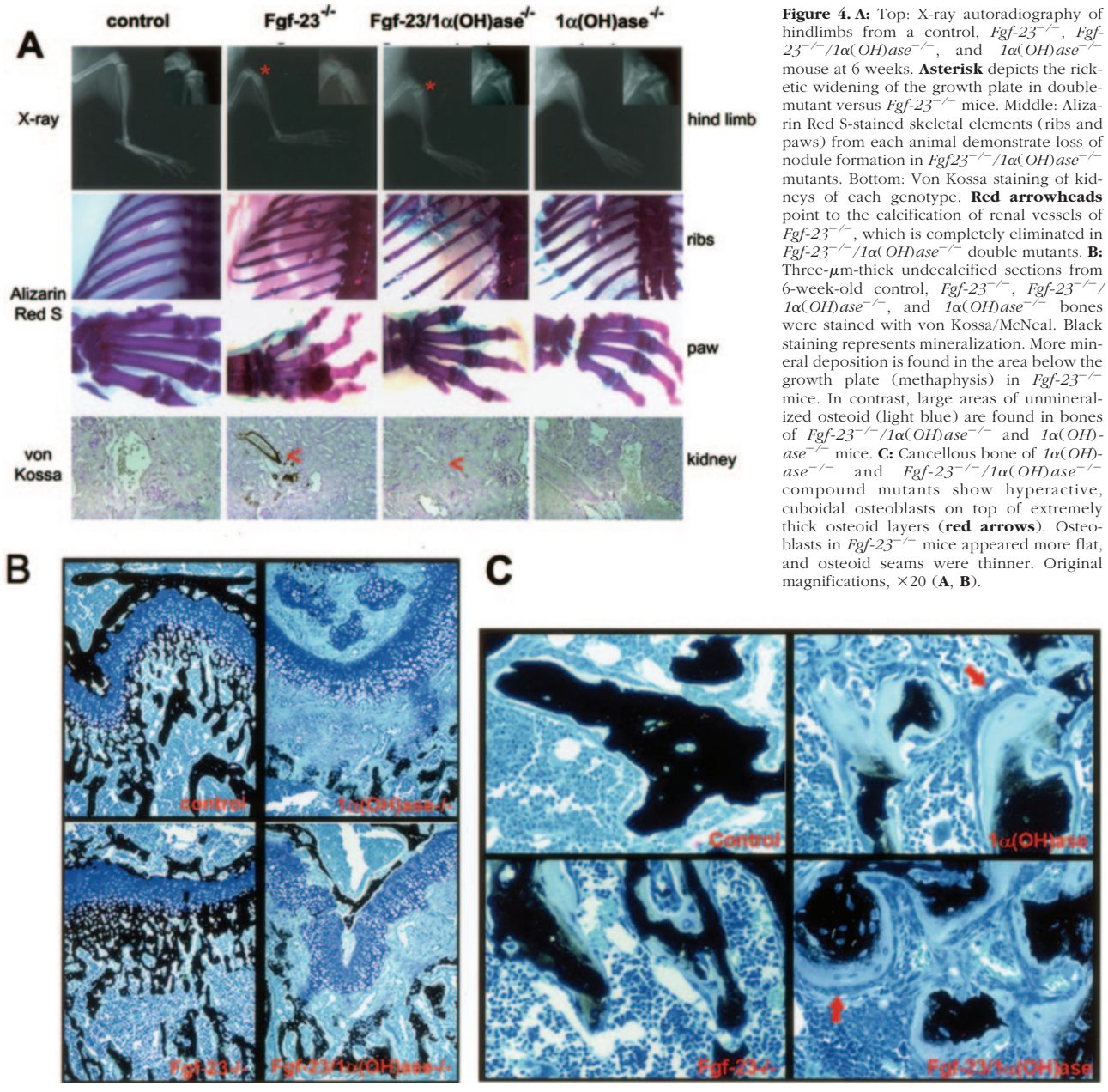

Figure 4. A: Top: X-ray autoradiography of hindlimbs from a control, *Fgf-23*$^{-/-}$, *Fgf-23*$^{-/-}$*/1α(OH)ase*$^{-/-}$, and *1α(OH)ase*$^{-/-}$ mouse at 6 weeks. **Asterisk** depicts the rickets widening of the growth plate in double-mutant versus *Fgf-23*$^{-/-}$ mice. Middle: Alizarin Red S-stained skeletal elements (ribs and paws) from each animal demonstrate loss of nodule formation in *Fgf23*$^{-/-}$*/1α(OH)ase*$^{-/-}$ mutants. Bottom: Von Kossa staining of kidneys of each genotype. **Red arrowheads** point to the calcification of renal vessels of *Fgf-23*$^{-/-}$, which is completely eliminated in *Fgf-23*$^{-/-}$*/1α(OH)ase*$^{-/-}$ double mutants. **B:** Three-μm-thick undecalcified sections from 6-week-old control, *Fgf-23*$^{-/-}$, *Fgf-23*$^{-/-}$*/1α(OH)ase*$^{-/-}$, and *1α(OH)ase*$^{-/-}$ bones were stained with von Kossa/McNeal. Black staining represents mineralization. More mineral deposition is found in the area below the growth plate (methaphysis) in *Fgf-23*$^{-/-}$ mice. In contrast, large areas of unmineralized osteoid (light blue) are found in bones of *Fgf-23*$^{-/-}$*/1α(OH)ase*$^{-/-}$ and *1α(OH)ase*$^{-/-}$ mice. **C:** Cancellous bone of *1α(OH)ase*$^{-/-}$ and *Fgf-23*$^{-/-}$*/1α(OH)ase*$^{-/-}$ compound mutants show hyperactive, cuboidal osteoblasts on top of extremely thick osteoid layers (**red arrows**). Osteoblasts in *Fgf-23*$^{-/-}$ mice appeared more flat, and osteoid seams were thinner. Original magnifications, ×20 (**A**, **B**).

typical features of rickets such as widening of epiphysis, resembling the *1α(OH)ase*$^{-/-}$phenotype (Figure 4A).

To further determine the mineralization pattern of long bones, methylmethacrylate sections from 6-week-old mice were prepared for histological examination. Femurs of *Fgf-23*$^{-/-}$ mice showed narrowed growth plates with decreased numbers of hypertrophic cells and more mineral deposition in the primary spongiosa immediately adjacent to the hypertrophic chondrocytes when compared with wild type. Interestingly, the histology observed in *Fgf-23*$^{-/-}$*/1α(OH)ase*$^{-/-}$ double mutants was characterized by widened growth plates with increased numbers of hypertrophic chondrocytes, a marked decline in mineral deposition in trabecular bone, and accumulation of unmineralized osteoid, mimicking the ricketic features found in *1α(OH)ase*$^{-/-}$ animals (Figure 4B). Cancellous bone in both *1α(OH)ase*$^{-/-}$ and compound mutants showed hyperactive, cuboidal osteoblasts on top of extremely thick osteoid layers. In contrast, osteoblasts in *Fgf-23*$^{-/-}$ mice appeared more flat, and osteoid seams were thinner compared with *1α(OH)ase*$^{-/-}$ mice and compound mutants (Figure 4C). Quantitative histomorphometry was performed to confirm the impaired bone mineralization and to demonstrate the increase in osteoid volume in all groups of mutant mice, especially

Table 1. Peripheral Quantitative Computed Tomography Data in the Various Genotypes

Variable	Control	*Fgf-23*$^{-/-}$	*Fgf-23*$^{-/-}$/*1α(OH)ase*$^{-/-}$	*1α(OH)ase*$^{-/-}$
Femoral metaphysis				
Total BMD (mg/cm^3)	384.9 ± 26.4	290.0 ± 25.2	187.7 ± 0.9	182.7 ± 4.66
Cortical/subcortical BMD (mg/cm^3)	621.7 ± 18.4	435.3 ± 76	333.7 ± 40.1	417.8 ± 41.4
Trabecular BMD (mg/cm^3)	215.9 ± 33.5	200.4 ± 1.1	101.7 ± 17.2	81.5 ± 6.9
Femoral shaft				
Total BMD (mg/cm^3)	462.8 ± 18.5	359.6 ± 22.4	230.2 ± 12.8	282 ± 20.7
Total area (cm^2)	1.73 ± 0.05	1.28 ± 0.03	1.17 ± 0.23	1.09 ± 0.07
Cortical area (cm^2)	0.658 ± 0.027	0.36 ± 0.06	0.125 ± 0.035	0.163 ± 0.04
Cortical thickness (mm)	0.158 ± 0.005	0.098 ± 0.02	0.035 ± 0.014	0.046 ± 0.011

1α(OH)ase$^{-/-}$ and *Fgf-23*$^{-/-}$/*1α(OH)ase*$^{-/-}$ double mutants (Figure 2E). Furthermore, pQCT analyses of the femoral methaphysis and femoral shaft were performed to complement the histological analyses (Table 1).

Gene Expression

To analyze the differentiation status of bone cells, we performed *in situ* hybridization on paraffin sections prepared from tibia of control, *Fgf-23*$^{-/-}$, *Fgf-23/1α(OH)ase*$^{-/-}$, and *1α(OH)ase*$^{-/-}$ littermates at 6 weeks of age (Figure 5). We were able to confirm the reduced number of hypertrophic chondrocytes in *Fgf-23*$^{-/-}$ animals,[9] when compared with control mice, as demonstrated by the marked decrease in collagen type X expression, a marker for hypertrophic cells. In contrast, we noted a marked increase of collagen type X-positive cell layers in *Fgf-23/1α(OH)ase*$^{-/-}$ double mutants, resembling the phenotype of *1α(OH)ase*$^{-/-}$ animals. In addition, expression of collagen type II emphasized the presence of unstained hypertrophic chondrocytes in the growth plate of double and *1α(OH)ase*$^{-/-}$ single mutants, a characteristic feature that was never apparent in control or *Fgf-23*$^{-/-}$ animals, suggesting the presence of ricketic phenotypes in both *1α(OH)ase*$^{-/-}$ and *Fgf-23/1α(OH)ase*$^{-/-}$ mouse strains. We also examined expression of osteopontin, a marker for late hypertrophic chondrocytes and early osteoblasts, and found a relative increase in the expression of osteopontin in osteoblasts of *Fgf-23*$^{-/-}$ mice, suggesting accelerated bone formation.[9] The expression of osteopontin in *Fgf-23/1α(OH)ase*$^{-/-}$ bones appeared to be reduced similarly as observed in *1α(OH)ase*$^{-/-}$ mice. Matrix gla protein, a marker for resting, proliferating, and late hypertrophic chondrocytes, seemed to be more strongly expressed in the growth plate of *1α(OH)ase*$^{-/-}$ and *Fgf-23*$^{-/-}$/*1α(OH)ase*$^{-/-}$ double mutants, suggesting an inhibition of mineralization in these bones.

Discussion

Although maintenance of calcium and phosphate homeostasis is of crucial biological importance, the precise mechanisms of phosphate homeostasis are not yet fully understood. As for calcium, it is well accepted that PTH, $1,25(OH)_2D_3$, and calcium-sensing receptors co-ordinately regulate calcium homeostasis.[38] In contrast to the conventional notion that phosphate homeostasis is passively mediated by the molecules that are involved in regulating calcium homeostasis, serum calcium and PTH levels are usually normal in patients with X-linked hypophosphatemia, autosomal dominant hypophosphatemic rickets, and tumor-induced osteomalacia, despite the presence of severe hypophosphatemia, and

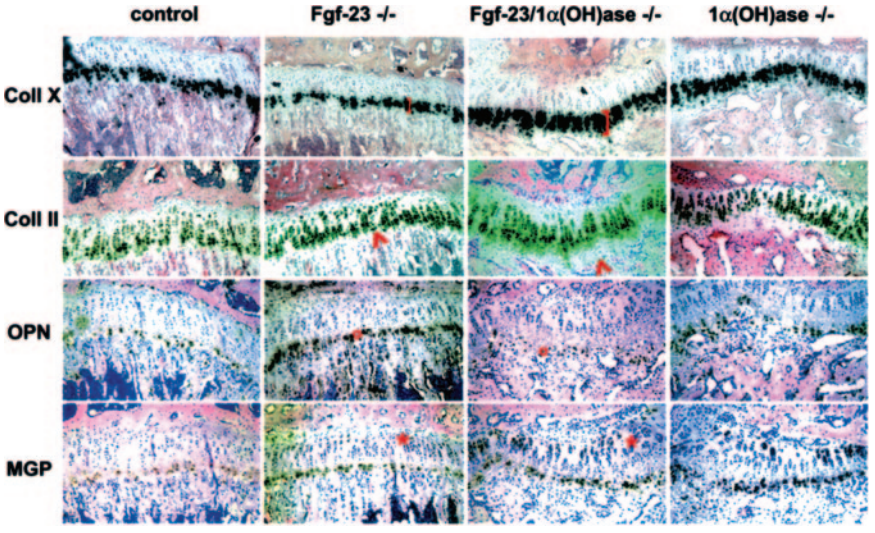

Figure 5. *In situ* hybridization with riboprobes for collagen type X (Coll X), collagen type II (Coll II), osteopontin (OPN), and matrix gla protein (MGP) on sections from tibia of control, *Fgf-23*$^{-/-}$, *Fgf-23*$^{-/-}$/*1α(OH)ase*$^{-/-}$, and *1α(OH)ase*$^{-/-}$ at 6 weeks. Brackets depict the size of the zone of hypertrophic chondrocytes. **Red arrowheads** point to an area of hypertrophic chondrocytes that is only present in *Fgf-23*$^{-/-}$/*1α(OH)ase*$^{-/-}$ and *1α(OH)ase*$^{-/-}$ bones. **Red circles** show the decrease in OPN expression in the ricketic phenotype, and **red asterisk** depicts an expansion of MGP expression in the growth plate of *Fgf-23*$^{-/-}$/*1α(OH)ase*$^{-/-}$ and *1α(OH)ase*$^{-/-}$ bones.

renal phosphate wasting, suggesting the existence of a novel phosphate-regulating pathway independent of classic calcium-regulating pathways. Subsequent studies of such rare genetic diseases have identified FGF-23 as a phosphaturic factor. Mutations in the *FGF-23* gene were identified as cause for autosomal dominant hypophosphatemic rickets[3]; furthermore, FGF-23 was shown to be the responsible humoral factor in tumor-induced osteomalacia,[2] and elevated levels of FGF-23 were detected in patients with X-linked hypophosphatemia.[39,40] Moreover, administration of FGF-23 could induce urinary phosphate excretion by suppressing renal expression of sodium-phosphate co-transporters.[25] All these studies suggest that increased FGF-23 activity leads to hypophosphatemia and hyperphosphaturia.

Our understanding of the bioactivities of FGF-23 is significantly enhanced by the generation of genetically altered *Fgf-23* mouse models; transgenic mice exhibit hypophosphatemia, and hyperphosphaturia, without significantly affecting serum calcium and $1,25(OH)_2D_3$ levels,[5–7] whereas *Fgf-23*$^{-/-}$ mice showed hyperphosphatemia, and elevated serum level of $1,25(OH)_2D_3$.[8,9] The phenotype of *Fgf-23*$^{-/-}$ animals is analogous to patients with familial tumoral calcinosis, characterized by elevated serum phosphate levels, which are caused by missense mutations in the *FGF-23* gene.[10,12] Other issues that are not yet clearly understood are the *in vivo* interaction between FGF-23 and vitamin D and whether skeletal abnormalities detected in *Fgf-23*$^{-/-}$ animals are a vitamin D-mediated process. To address such unresolved questions, we have generated *Fgf-23*$^{-/-}$/*1α(OH)ase*$^{-/-}$ compound mutants. Most of the skeletal and soft tissue phenotypes detected in *Fgf-23*$^{-/-}$ mice[9] were reversed in double-mutant animals; these include but are not limited to the disappearance of abnormal skeletal nodule formation and soft tissue calcifications in *Fgf-23*$^{-/-}$*/1α(OH)ase*$^{-/-}$ mutants, suggesting that at least some of the anomalies found in *Fgf-23*$^{-/-}$ mice are mediated through increased vitamin D activities. In addition, loss of vitamin D activities from *Fgf-23*$^{-/-}$ mice reverses severe hyperphosphatemia to hypophosphatemia, possibly attributable to hyperphosphaturia in *Fgf-23*$^{-/-}$*/1α(OH)ase*$^{-/-}$ mice. An *in vivo* inverse correlation between the expression of *Fgf-23* and *NaPi2a* has been well documented both in *Fgf-23*$^{-/-}$ mice and *FGF23* transgenic mice. In contrast to the decreased renal expression of NaPi2a protein in *FGF23* transgenic mice,[5–7] an increased expression of NaPi2a protein is documented in *Fgf-23*$^{-/-}$ mice (Figure 3F).[8,9] Compared with the *Fgf-23*$^{-/-}$ mice, our immunostaining data demonstrated a markedly decreased renal expression of NaPi2a protein in *Fgf-23*$^{-/-}$*/1α(OH)ase*$^{-/-}$ and *1α(OH)ase*$^{-/-}$ mice (Figure 3F), suggesting that the hyperphosphaturia in *Fgf-23*$^{-/-}$*/1α(OH)ase*$^{-/-}$ and *1α(OH)ase*$^{-/-}$ (Figure 3D) mice is probably attributable to the down-regulation of NaPi2a. Moreover, we found that serum phosphate levels in *Fgf-23*$^{-/-}$*/NaPi2a*$^{-/-}$ and *NaPi2a*$^{-/-}$ mutant mice were similar to the ones found in *Fgf-23*$^{-/-}$*/1α(OH)ase*$^{-/-}$ and *1α(OH)ase*$^{-/-}$ mice, suggesting that the hypophosphatemia in *Fgf-23*$^{-/-}$/*1α(OH)ase*$^{-/-}$ is mainly attributable to a reduction in renal phosphate reabsorption (Figure 3C). Further studies, however, are needed to determine roles of other renal and intestinal NaPi co-transporters, including NaPi2c in these mice.

Another aspect that needs further study is to determine whether increased levels of PTH in *Fgf-23*$^{-/-}$/*1α(OH)ase*$^{-/-}$ compound mutants could partly ameliorate some of the abnormal phenotypes of *Fgf-23*$^{-/-}$mice. We believe that the decreased activity of NaPi2a in *Fgf-23*$^{-/-}$*/1α(OH)ase*$^{-/-}$ double-knockout mice is partly regulated by the elevated serum PTH levels. Our preliminary observations suggest that altered phosphate homeostasis in *Fgf-23*$^{-/-}$ mice is indeed regulated by NaPi2a, as demonstrated by increased expression of NaPi2a in *Fgf-23*$^{-/-}$ mice, and by reversing the phosphate homeostasis in *Fgf-23*$^{-/-}$ mice by genetically ablating NaPi2a from these mice (*Fgf-23*$^{-/-}$*/NaPi2a*$^{-/-}$ double-knockout mice). Earlier studies have shown an inverse correlation between PTH and renal expression of NaPi2a[8]; taking into consideration our results of increased serum level of PTH and decreased renal expression of NaPi2a in *Fgf-23*$^{-/-}$*/1α(OH)ase*$^{-/-}$ mice, we speculate that the high levels of PTH might have suppressive effects on NaPi2a. In contrast to the *Fgf-23*$^{-/-}$ mice, in which markedly increased serum $1,25(OH)_2D_3$ levels are associated with increased renal expression of 1α(OH)ase,[8,9] earlier studies have reported that FGF-23 could reduce $1,25(OH)_2D_3$ levels by suppressing the renal expression of 1α(OH)ase and inducing 24-hydroxylase [24(OH)ase] in mice treated with recombinant FGF-23.[25] The interaction between FGF-23 and vitamin D is a rather complex process,[41,42] and a single injection of $1,25(OH)_2D_3$ can increase serum levels of Fgf-23 in normal mice.[25] A separate study demonstrated a dose-dependent effect of $1,25(OH)_2D_3$ on circulating Fgf-23, which was independent of serum levels of phosphate, both in normal and thyroid-parathyroidectomized rats.[29] Studies have also suggested a vitamin D-independent activity of Fgf-23. For instance, a rapid bolus intravenous injection of FGF-23 to the *VDR*$^{-/-}$ mice could further decrease serum phosphate levels and reduce renal expression of sodium phosphate co-transporter type IIa (NaPi2a) and 1α(OH)ase.[43] Similarly, *VDR*$^{-/-}$ mice, which exhibit undetectable serum levels of Fgf-23 with severe hypophosphatemia, fed a rescue diet showed restored serum phosphate levels and elevated serum Fgf-23 levels,[44] concluding that production of Fgf-23 in response to phosphate changes is not a vitamin D-dependent process. In a separate study, Inoue and colleagues[45] have shown that injection of naked DNA encoding the human FGF-23 (R179Q) into *VDR*$^{-/-}$ mice could lower renal phosphate transport and expression of *1α(OH)ase*, in a vitamin D-independent manner; in contrast, the induction of 24(OH)ase and reduction of serum $1,25(OH)_2D_3$ by FGF-23 is a vitamin D-mediated process. Based on the results of our current *in vivo* genetic manipulation study and earlier studies, it appears likely that a feedback loop between $1,25(OH)_2D_3$ and FGF-23 delicately regulates phosphate homeostasis and skeletogenesis.[37]

Both *Fgf-23* transgenic and knockout mice have shown abnormal skeletal phenotypes,[5–9] but it remained uncer-

tain whether these skeletal alterations are because of direct effects of Fgf-23 on bone or simply related to changes in phosphate homeostasis. In this study, we have shown that normal osteocytes are the main *Fgf-23*-expressing cells in adult mice; likewise, an increased expression of *Fgf-23* was detected at sites of new bone formation because of fractures.[46] Such observations make it plausible that Fgf-23 is directly involved in normal skeletogenesis, which is again supported by the fact that *Fgf-23*$^{-/-}$ mice have significantly reduced BMD (Figure 2, C and D). It thus appears likely that Fgf-23, locally produced by osteocytes through a yet unknown paracrine/autocrine signaling mechanism, controls skeletogenesis. However, in the absence of $1,25(OH)_2D_3$, the bone phenotype of *Fgf-23*$^{-/-}$/*1α(OH)ase*$^{-/-}$ double mutants was similar to *1α(OH)ase*$^{-/-}$ mice (Figures 2 and 4), suggesting that the presence or absence of Fgf-23 does not have a major impact on skeletal phenotypes of *1α(OH)ase*$^{-/-}$ mice. On the other hand, the very high PTH serum levels in *1α(OH)ase*$^{-/-}$ and in *Fgf-23*$^{-/-}$/*1α(OH)ase*$^{-/-}$ compound mice may override any more subtle additional defects induced by Fgf-23 deficiency.

Ablation of *1α(OH)ase* function in *Fgf-23*$^{-/-}$ mice not only reversed hyperphosphatemia and hypercalcemia but, more importantly, completely eliminated the extensive soft tissue calcifications found in *Fgf-23*$^{-/-}$ mice (Figure 4A). These findings suggest that lack of *Fgf-23*, through a negatively regulated circuit of $1,25(OH)_2D_3$ synthesis, is involved in the pathogenesis of abnormal soft tissue calcifications.

In conclusion, we have shown a pathological role of vitamin D in altered phosphate homeostasis, skeletogenesis, and ectopic calcifications in *Fgf-23*$^{-/-}$ mice.

Acknowledgments

We thank Da Chang, Somi Kim, and Stephelynn DeLuca for technical support. We are also very grateful to the histology core of the Endocrine Unit at the MGH for their support.

References

1. Bringhurst FR, Demay MB, Kronenberg HM: Hormones and disorders of mineral metabolism. Williams Textbook of Endocrinology. Philadelphia, WB Saunders Co., 1998, pp 1155–1210
2. Shimada T, Mizutani S, Muto T, Yoneya T, Hino R, Takeda S, Takeuchi Y, Fujita T, Fukumoto S, Yamashita T: Cloning and characterization of FGF23 as a causative factor of tumor-induced osteomalacia. Proc Natl Acad Sci USA 2001, 98:6500–6505
3. White KE, Evans WE, O'Riordan JLH, Speer MC, Econs MJ, Lorenz-Depiereux B, Grabowski M, Mettinger T, Strom TM: Autosomal dominant hypophosphataemic rickets is associated with mutations in FGF23. The ADHR Consortium. Nat Genet 2000, 26:345–348
4. Francis F, Henning S, Korn B, Reinhardt R, de Jong P, Poustka A, Lehrach H, Rowe PSN, Goulding JN, Summerfield T, Mountford R, Read AP, Popowska E, Pronicka E, Davies KE, O'Riordan JLH, Econs MJ, Nesbitt T, Drezner MK, Oudet C, Pannetier S, Hanauer A, Strom TM, Meindl A, Lorenz B, Cagnoli M, Mohnike KL, Murken J, Meitinger T: A gene (PEX) with homologies to endopeptidases is mutated in patients with X-linked hypophosphatemic rickets. The HPY Consortium. Nat Genet 1995, 11:130–136
5. Shimada T, Urakawa I, Yamazaki Y, Hasegawa H, Hino R, Yoneya T, Takeuchi Y, Fujita T, Fukumoto S, Yamashita T: FGF-23 transgenic mice demonstrate hypophosphatemic rickets with reduced expression of sodium phosphate cotransporter type IIa. Biochem Biophys Res Commun 2004, 314:409–414
6. Larsson T, Marsell R, Schipani E, Ohlsson C, Ljunggren O, Tenenhouse HS, Juppner H, Jonsson KB: Transgenic mice expressing fibroblast growth factor 23 under the control of the {alpha}1(I) collagen promoter exhibit growth retardation, osteomalacia and disturbed phosphate homeostasis. Endocrinology 2004, 145:3087–3094
7. Bai X, Miao D, Li J, Goltzman D, Karaplis AC: Transgenic mice overexpressing human fibroblast growth factor 23(R176Q) delineate a putative role for parathyroid hormone in renal phosphate wasting disorders. Endocrinology 2004, 145:5269–5279
8. Shimada T, Kakitani M, Yamazaki Y, Hasegawa H, Takeuchi Y, Fujita T, Fukumoto S, Tomizuka K, Yamashita T: Targeted ablation of Fgf23 demonstrates an essential physiological role of FGF23 in phosphate and vitamin D metabolism. J Clin Invest 2004, 113:561–568
9. Sitara D, Razzaque MS, Hesse M, Yoganathan S, Taguchi T, Erben RG, Jueppner H, Lanske B: Homozygous ablation of fibroblast growth factor-23 results in hyperphosphatemia and impaired skeletogenesis, and reverses hypophosphatemia in Phex-deficient mice. Matrix Biol 2004, 23:421–432
10. Larsson T, Yu X, Davis SI, Draman MS, Mooney SD, Cullen MJ, White KE: A novel recessive mutation in fibroblast growth factor-23 causes familial tumoral calcinosis. J Clin Endocrinol Metab 2005, 90:2424–2427
11. Topaz O, Bergman R, Mandel U, Maor G, Goldberg R, Richard G, Sprecher E: Absence of intraepidermal glycosyltransferase ppGalNac-T3 expression in familial tumoral calcinosis. Am J Dermatopathol 2005, 27:211–215
12. Benet-Pages A, Orlik P, Strom TM, Lorenz-Depiereux B: An FGF23 missense mutation causes familial tumoral calcinosis with hyperphosphatemia. Hum Mol Genet 2005, 14:385–390
13. Frishberg Y, Topaz O, Bergman R, Behar D, Fisher D, Gordon D, Richard G, Sprecher E: Identification of a recurrent mutation in GALNT3 demonstrates that hyperostosis-hyperphosphatemia syndrome and familial tumoral calcinosis are allelic disorders. J Mol Med 2005, 83:33–38
14. Ichikawa S, Lyles KW, Econs MJ: A novel GALNT3 mutation in a pseudoautosomal dominant form of tumoral calcinosis: evidence that the disorder is autosomal recessive. J Clin Endocrinol Metab 2005, 90:2420–2423
15. Erben RG, Soegiarto DW, Weber K, Zeitz U, Lieberherr M, Gniadecki R, Moller G, Adamski J, Balling R: Deletion of deoxyribonucleic acid binding domain of the vitamin D receptor abrogates genomic and nongenomic functions of vitamin D. Mol Endocrinol 2002, 16:1524–1537
16. Li YC, Pirro AE, Amling M, Delling G, Baron R, Bronson R, Demay MB: Targeted ablation of the vitamin D receptor: an animal model of vitamin D-dependent rickets type II with alopecia. Proc Natl Acad Sci USA 1997, 94:9831–9835
17. Yoshizawa T, Handa Y, Uematsu Y, Takeda S, Sekine K, Yoshihara Y, Kawakami T, Arioka K, Sato H, Uchiyama Y, Masushige S, Fukamizu A, Matsumoto T, Kato S: Mice lacking the vitamin D receptor exhibit impaired bone formation, uterine hypoplasia and growth retardation after weaning. Nat Genet 1997, 16:391–396
18. Panda DK, Miao D, Bolivar I, Li J, Huo R, Hendy GN, Goltzman D: Inactivation of the 25-hydroxyvitamin D 1alpha-hydroxylase and vitamin D receptor demonstrates independent and interdependent effects of calcium and vitamin D on skeletal and mineral homeostasis. J Biol Chem 2004, 279:16754–16766
19. Dardenne O, Prud'homme J, Arabian A, Glorieux FH, St-Arnaud R: Targeted inactivation of the 25-hydroxyvitamin D(3)-1(alpha)-hydroxylase gene (CYP27B1) creates an animal model of pseudovitamin D-deficiency rickets. Endocrinology 2001, 142:3135–3141
20. Ladhani S, Srinivasan L, Buchanan C, Allgrove J: Presentation of vitamin D deficiency. Arch Dis Child 2004, 89:781–784
21. Dardenne O, Prudhomme J, Hacking SA, Glorieux FH, St-Arnaud R: Rescue of the pseudo-vitamin D deficiency rickets phenotype of CYP27B1-deficient mice by treatment with 1,25-dihydroxyvitamin D3: biochemical, histomorphometric, and biomechanical analyses. J Bone Miner Res 2003, 18:637–643
22. Dardenne O, Prud'homme J, Glorieux FH, St-Arnaud R: Rescue of the

phenotype of CYP27B1 (1alpha-hydroxylase)-deficient mice. J Steroid Biochem Mol Biol 2004, 89–90:327–330
23. St-Arnaud R, Dardenne O, Prud'homme J, Hacking SA, Glorieux FH: Conventional and tissue-specific inactivation of the 25-hydroxyvitamin D-1alpha-hydroxylase (CYP27B1). J Cell Biochem 2003, 88:245–251
24. Fukumoto S, Matsumoto T, Yamoto H, Kawashima H, Ueyama Y, Tamaoki N, Ogata E: Suppression of serum 1,25-dihydroxyvitamin D in humoral hypercalcemia of malignancy is caused by elaboration of a factor that inhibits renal 1,25-dihydroxyvitamin D3 production. Endocrinology 1989, 124:2057–2062
25. Shimada T, Hasegawa H, Yamazaki Y, Muto T, Hino R, Takeuchi Y, Fujita T, Nakahara K, Fukumoto S, Yamashita T: FGF-23 is a potent regulator of vitamin D metabolism and phosphate homeostasis. J Bone Miner Res 2004, 19:429–435
26. Tenenhouse H: Investigation of the mechanism for abnormal renal 25-hydroxyvitamin D^3-1-hydroxylase activity in the X-linked Hyp mouse. Endocrinology 1984, 115:634–639
27. Meyer Jr RA, Meyer MH, Gray RW, Bruns ME: Evidence that low plasma 1,25-dihydroxyvitamin D causes intestinal malabsorption of calcium and phosphate in juvenile X-linked hypophosphatemic mice. J Bone Miner Res 1987, 2:67–82
28. Malloy PJ, Xu R, Peng L, Peleg S, Al-Ashwal A, Feldman D: Hereditary 1,25-dihydroxyvitamin D resistant rickets due to a mutation causing multiple defects in vitamin D receptor function. Endocrinology 2004, 145:5106–5114
29. Saito H, Maeda A, Ohtomo S, Hirata M, Kusano K, Kato S, Ogata E, Segawa H, Miyamoto K, Fukushima N: Circulating FGF-23 is regulated by 1alpha,25-dihydroxyvitamin D3 and phosphorus in vivo. J Biol Chem 2005, 280:2543–2549
30. Eicher E, Southard J, Scriver C, Glorieux F: Hypophosphatemia: mouse model for human familial hypophosphataemic (vitamin D-resistant) rickets. Proc Natl Acad Sci USA 1976, 73:4667–4671
31. Dardenne O, Prud'homme J, Hacking SA, Glorieux FH, St-Arnaud R: Correction of the abnormal mineral ion homeostasis with a high-calcium, high-phosphorus, high-lactose diet rescues the PDDR phenotype of mice deficient for the 25-hydroxyvitamin D-1alpha-hydroxylase (CYP27B1). Bone 2003, 32:332–340
32. Beck L, Karaplis AC, Amizuka N, Hewson AS, Ozawa H, Tenenhouse HS: Targeted inactivation of Npt2 in mice leads to severe renal phosphate wasting, hypercalciuria, and skeletal abnormalities. Proc Natl Acad Sci USA 1998, 95:5372–5377
33. McLeod MJ: Differential staining of cartilage and bone in whole mouse fetuses by alcian blue and alizarin red S. Tetratology 1980, 22:299–301
34. Lanske B, Divieti P, Kovacs CS, Pirro A, Landis WJ, Krane SM, Bringhurst FR, Kronenberg HM: The parathyroid hormone (PTH)/PTH-related peptide receptor mediates actions of both ligands in murine bone. Endocrinology 1998, 139:5194–5204
35. Schenk R, Olah A, Herrmann W: Preparation of calcified tissues for light microscopy. Methods of Calcified Tissue Preparation. Edited by G Dickson. Amsterdam, Elsevier, 1984, pp 1–56
36. Razzaque MS, Foster CS, Ahmed AR: Role of collagen-binding heat shock protein 47 and transforming growth factor-beta1 in conjunctival scarring in ocular cicatricial pemphigoid. Invest Ophthalmol Vis Sci 2003, 44:1616–1621
37. Razzaque MS, Sitara D, Taguchi T, St-Arnaud R, Lanske B: Premature ageing-like phenotype in fibroblast growth factor 23 null mice is a vitamin-D mediated process. FASEB J 2006, 20:720–722
38. Brown EM, Gamba G, Riccardi D, Lombardi M, Butters R, Kifor O, Sun A, Hediger MA, Lytton J, Hebert SC: Cloning and characterization of an extracellular Ca(2+)-sensing receptor from bovine parathyroid. Nature 1993, 366:575–580
39. Yamazaki Y, Okazaki R, Shibata M, Hasegawa Y, Satoh K, Tajima T, Takeuchi Y, Fujita T, Nakahara K, Yamashita T, Fukumoto S: Increased circulatory level of biologically active full-length FGF-23 in patients with hypophosphatemic rickets/osteomalacia. J Clin Endocrinol Metab 2002, 87:4957–4960
40. Jonsson KB, Zahradnik R, Larsson T, White KE, Sugimoto T, Imanishi Y, Yamamoto T, Hampson G, Koshiyama H, Ljunggren O, Oba K, Yang IM, Miyauchi A, Econs MJ, Lavigne J, Juppner H: Fibroblast growth factor 23 in oncogenic osteomalacia and X-linked hypophosphatemia. N Engl J Med 2003, 348:1656–1663
41. Razzaque MS, St-Arnaud R, Taguchi T, Lanske B: FGF-23, vitamin D and calcification: the unholy triad. Nephrol Dial Transplant 2005, 20:2032–2035
42. Razzaque MS, Lanske B: Hypervitaminosis D and premature aging: lessons learned from Fgf23 and Klotho mutant mice. Trends Mol Med 2006, 12:298–305
43. Shimada T, Yamazaki Y, Takahashi M, Hasegawa H, Urakawa I, Oshima T, Ono K, Kakitani M, Tomizuka K, Fujita T, Fukumoto S, Yamashita T: Vitamin D receptor-independent FGF23 actions in regulating phosphate and vitamin D metabolism. Am J Physiol 2005, 289:F1088–F1095
44. Yu X, Sabbagh Y, Davis SI, Demay MB, White KE: Genetic dissection of phosphate- and vitamin D-mediated regulation of circulating Fgf23 concentrations. Bone 2005, 36:971–977
45. Inoue Y, Segawa H, Kaneko I, Yamanaka S, Kusano K, Kawakami E, Furutani J, Ito M, Kuwahata M, Saito H, Fukushima N, Kato S, Kanayama HO, Miyamoto KI: Role of vitamin D receptor on FGF23 action in phosphate metabolism. Biochem J 2005, 390:325–331
46. Riminucci M, Collins MT, Fedarko NS, Cherman N, Corsi A, White KE, Waguespack S, Gupta A, Hannon T, Econs MJ, Bianco P, Gehron Robey P: FGF-23 in fibrous dysplasia of bone and its relationship to renal phosphate wasting. J Clin Invest 2003, 112:683–692